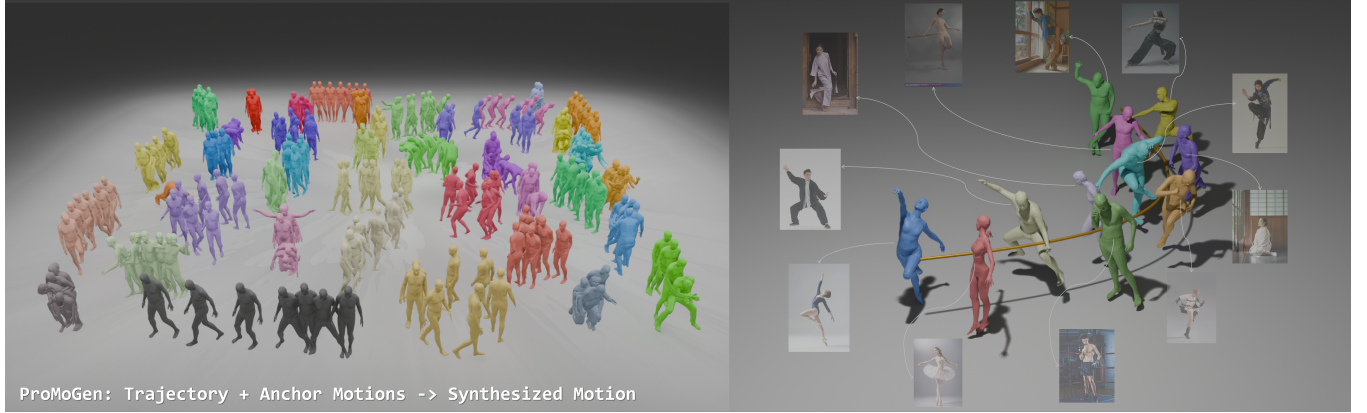


# PMG: Progressive Motion Generation via Sparse Anchor Postures Curriculum Learning

Yingjie Xi  
yxi@bournemouth.ac.uk  
Bournemouth University  
Bournemouth, Dorset, UK

Jian Jun Zhang  
jzhang@bournemouth.ac.uk  
Bournemouth University  
Bournemouth, Dorset, UK

Xiaosong Yang  
xyang@bournemouth.ac.uk  
Bournemouth University  
Bournemouth, Dorset, UK



**Figure 1:** The left panel illustrates the synthesized results of the ProMoGen framework, under the control of both predefined trajectory and arbitrary anchor motions. The right panel delineates the inference process of our framework, wherein specific poses extracted from various images, as anchor motions, are combined with a predefined trajectory to synthesize realistic and customized human motion.

## Abstract

In computer animation, game design, and human-computer interaction, synthesizing human motion that aligns with user intent remains a significant challenge. Existing methods have notable limitations: textual approaches offer high-level semantic guidance but struggle to describe complex actions accurately; trajectory-based techniques provide intuitive global motion direction yet often fall short in generating precise or customized character movements; and anchor poses-guided methods are typically confined to synthesize only simple motion patterns. To generate more controllable and precise human motions, we propose **ProMoGen (Progressive Motion Generation)**, a novel framework that integrates trajectory guidance with sparse anchor motion control. Global trajectories ensure consistency in spatial direction and displacement, while sparse anchor motions only deliver precise action guidance without displacement. This decoupling enables independent refinement of both aspects, resulting in a more controllable, high-fidelity, and sophisticated motion synthesis. ProMoGen supports both dual and single control paradigms within a unified training process. Moreover, we recognize that direct learning from sparse motions is inherently unstable, we introduce **SAP-CL (Sparse Anchor Posture Curriculum Learning)**, a curriculum learning strategy that progressively adjusts the number of anchors used for guidance, thereby enabling more precise and stable convergence. Extensive experiments demonstrate that ProMoGen excels in synthesizing vivid and diverse motions guided by predefined trajectory and

arbitrary anchor frames. Our approach seamlessly integrates personalized motion with structured guidance, significantly outperforming state-of-the-art methods across multiple control scenarios. <https://github.com/2022yingjie/ProMoGen.git>

## CCS Concepts

• **Computer systems organization** → **Embedded systems**; *Redundancy*; Robotics; • **Networks** → Network reliability.

## Keywords

Animation, Human Motion, Motion Synthesis, Generative Models, Curriculum Learning

## 1 Introduction

Human motion synthesis plays a crucial role in the field of cinematic character animation, game design, human-robot interaction, and virtual avatars. In these domains, there is a growing need for methods that can produce high-fidelity, expressive motion that is both semantically and environmentally aligned with specific thematic styles, while maintaining flexibility to accommodate diverse user requirements and interaction scenarios. Therefore, achieving precise control over motion trajectories and character postures is necessary to keep the generated motion realistic and desired.

Traditional human motion synthesis methods primarily include text-to-motion [4, 5, 11, 21, 32, 33, 38, 45, 48, 53, 58] synthesis, trajectory-to-motion synthesis [17, 24, 47], and audio-based synthesis [6, 47, 61, 63], which have enabled coarse alignment between

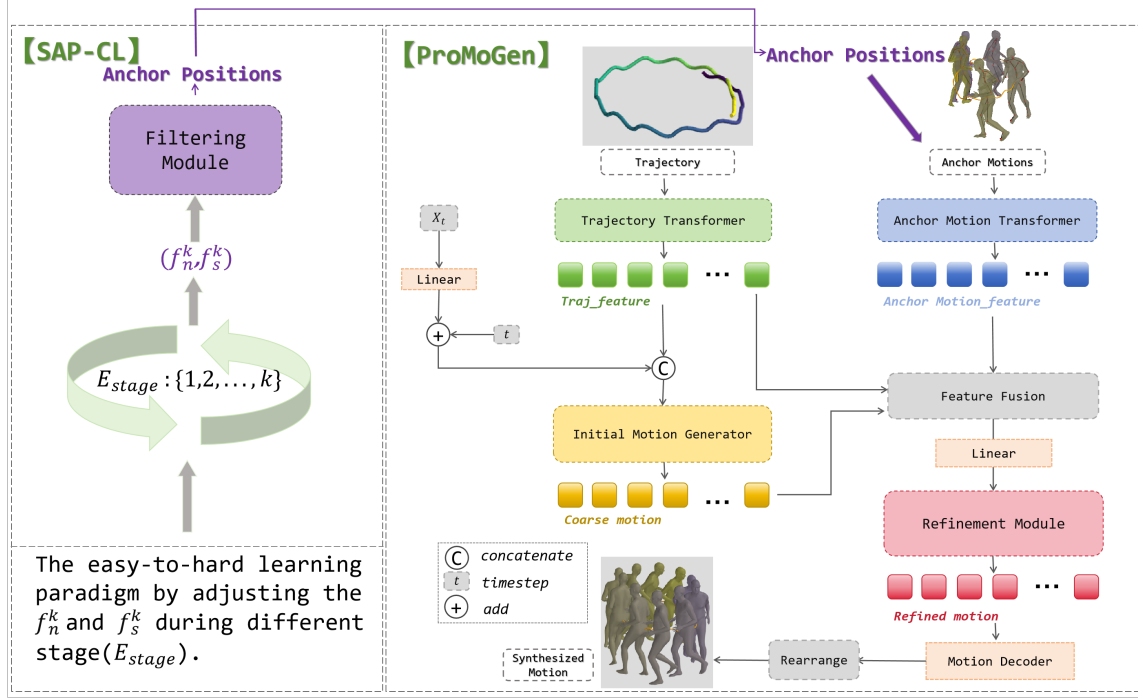


Figure 2: The SAP-CL training strategy(left panel) and the structure of ProMoGen method(right panel).

these conditions inputs and the generated motions. While these approaches are capable of generating smooth and simple human motion sequences, they still face significant challenges in producing highly customized or personalized complex motions that meet user-specific requirements [14]. For example, the specific posture at the selected position on the trajectory is the key to personalized motion expression, and this posture is often difficult to accurately describe using conventional text and other conditions. This limitation arises not only from the distribution of existing datasets, which tend to focus on simple motion patterns, but also from more fundamental issues, that the semantic ambiguity inherent in text descriptions and the geometric sparsity of trajectory signals, therefore further loss the interaction ability with the practical environment [10, 33, 39]. These factors often fail to provide sufficient guidance for specifying fine-grained motion details, hindering the generation of more complex and personalized motion sequences. Other works [28, 52] adopts transformer-based end-to-end network to make an interpolation task for motion in-between, but directly end-to-end learning paradigm cannot learn motion distribution well, resulting low-fidelity and single synthesis. The [25] explores the interplay between text and trajectories, as well as text and anchor postures positions, but it did not effectively decouple these features nor achieve refined control over human motion generation.

To address these limitations, we propose ProMoGen(Progressive Motion Generation), a diffusion-based framework [19, 20, 42, 54]. By synergizing trajectory control with sparse anchor motions guidance, our method facilitates hierarchically controllable, customized, and precise motion synthesis. The key insight driving our approach is the decomposition of motion generation into two complementary

subspaces: a global trajectory that governs macroscopic movement patterns, and local poses that represent stylistic content, towards to more diverse and free motion combination with control of arbitrary trajectory or motions. Specifically, to ensure robust understanding of global trajectories, we design the global Trajectory Feature Encoder (TFE), a transformer-based [37, 46] architecture that projects user-defined trajectories into a latent space, capturing both temporal displacement and directional coherence. In parallel, to dynamically guide motion synthesis under varying key postures, we develop the anchor Filtering Module, which samples sparse anchor poses based on predefined temporal density and interval elasticity to get specific anchor pose controls. Then an Anchor Motion Encoder (AME) is introduced to learn features from the sparse pose conditions. To effectively integrate the outputs of these components, we design a Initial Motion Generator and Refinement Module, the former is responsible to build coarse motion under the control of trajectory only, to roughly align the latent representations of postures and trajectory, and the latter is to ensure smooth and high-fidelity interpolation while maintaining input pose original details. Besides, the diffusion process significantly enhances the synthesis capabilities of ProMoGen, enabling the generation of realistic and precisely controlled motions.

In addition, traditional training directly using sparse signals(e.g., less than 5% frame density) often results in unstable gradient propagation due to insufficient supervisory information, hindering effective learning. Moreover, models trained under the specific conditions may not generalize well to varying inference scenarios.

To alleviate this challenge, we introduce a novel training strategy, termed Sparse Anchor Posture Curriculum Learning (SAP-CL) [3, 29, 31, 35, 36, 43, 49, 57, 60, 62]. Intuitively, in this work, the tasks with denser anchor postures are simpler, enabling model easily handle the task by providing more informative supervisory signals, then gradually increase the difficulty level to get a better convergence. Following this easy-to-hard paradigm, our approach begins by utilizing denser anchor posture guidance. This allows the model to learn fundamental motion features with more supervision. Subsequently, we progressively reduce the density of anchor poses, enabling the model to adapt to more challenging, sparse conditions while maintaining generalization.

We conduct extensive experiments to evaluate the performance of ProMoGen across various metrics. The results demonstrate that ProMoGen produces smooth and visually appealing results, outperforming existing methods.

The main contributions of this work are as follows:

- We propose a multi-guidance task that is used to synthesize human motion under the control of global trajectory and local postures, exploring the interactions between these two signals.
- We introduce ProMoGen, a well-designed network that integrates trajectory guidance with sparse anchor postures, enabling the generation of more controllable, high-fidelity.
- We introduce SAP-CL(Sparse Anchor Posture Curriculum Learning), this approach implements an easy-to-hard paradigm, ensuring stable convergence and facilitating motion synthesis in various scenarios by progressively increasing task complexity.
- We evaluate ProMoGen on multiple datasets and different scenarios, showcasing its superior performance compared to existing baselines. Ablation studies further validate the effectiveness of our proposed architecture and training strategy design.

## 2 Related Work

### 2.1 Motion Generation

With Variational Autoencoders(VAEs) [15, 32, 33, 38, 44, 48, 58] and Diffusion models [1, 4, 5, 7, 11, 21, 45, 53] emerging, human motion generation has evolved significantly. Among these advanced works, the text-to-motion task is one of the most compelling research direction [64], it leverages natural language descriptions as prompt input to synthesize realistic and semantically aligned human motions. Despite these improvements, text-based methods still face challenges [41, 50, 51] in precisely controlling motion trajectories and fine-grained kinematic details. On the one hand, text-based methods often struggle with ambiguous [23, 26, 27, 30], leading to misaligned or overly generic motions. On the other hand, it is difficult to describe complex and delicate human movements without other prior input, let alone achieving highly personalized or customized motion synthesis. Trajectory based [2, 13, 17, 24, 40, 47, 59] methods are proposed to focus on generating motions conditioned on predefined spatial paths, offering more explicit control over the global movement of characters. But they primarily focus on coarse path alignment rather than fine-grained pose control. Additionally,

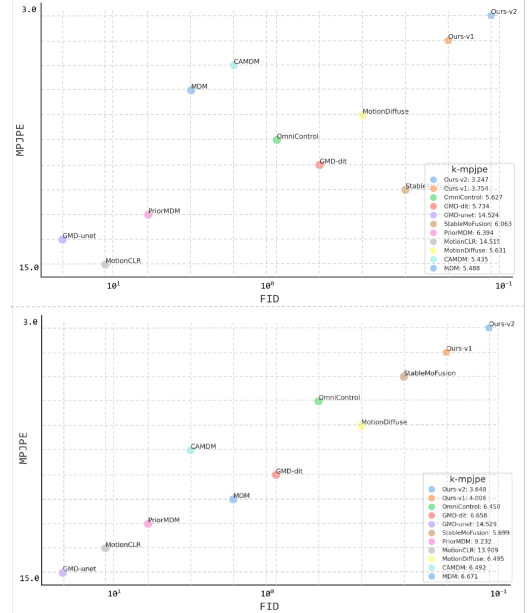


**Figure 3:** In this figure, the horizontal axis represents FID, while the vertical axis corresponds to MPJPE (To ensure comparability, the values of all models have been transformed to a uniform scale). Notably, data points that approach the upper right region along the diagonal indicate superior model performance. The v1 model achieves the most favorable results, thereby substantiating the robustness of our whole structure design. Additionally, the placement of v2 in the upper right corner further demonstrates the exceptional performance of our complete model with fine-designed components.

motion in-between [8, 9, 12, 22] focuses on generating complete motion sequences given key-frame poses.

We introduce ProMoGen, a novel framework for motion synthesis that synergistically exploits both trajectory information and anchor postures. By integrating these elements, ProMoGen offers explicit, robust global guidance alongside fine-grained local constraints, resulting in enhanced performance on complex, customized tasks. In contrast, prior approaches [25, 28] employ anchor conditioning through simple input masking or the provision of global positions. Such methods encourage models to learn merely an interpolation space rather than a deep understanding of the motion distribution and the intricate interplay between trajectories and postures. Our ProMoGen is diffusion-based, which could further dig the intricate connection between two conditions and have a better generation.

### 2.2 Curriculum learning

Directly learning from anchor postures of random arrangement is challenging due to the sparsity. A more effective strategy is to build a progressive paradigm, from easy to difficult. Curriculum Learning (CL) [3] has been proposed to implement this strategy in model training, it trains models by gradually introducing examples of increasing difficulty. CL has demonstrated its power in improving

the generalization capacity and convergence rate of various models in a wide range of scenarios such as computer vision [43, 57], natural language processing [29, 60, 62], robotics and medical applications [31, 35, 36, 49]. We introduce its thoughts into our work and design SAP-CL, an easy-to-hard paradigm to improve model convergence and resulting in high-quality and high-fidelity motion.

### 3 Method

In this section, we first provide an overview of the diffusion approach that underpins our methodology. Next, we detail the design of our network architecture, finally followed by an explanation of the curriculum learning strategy employed in our framework.

Let  $X_0$  represents the original motion, the  $\tau \in \mathbb{R}^{N \times 3}$  denote the predefined trajectory, where  $N$  represents the length of the motion sequence and the value 3 corresponds to the global coordinates of the human pelvis at each frame. In addition, let  $X_s \in \mathbb{R}^{M \times 6}$  denote the sparse anchor postures, where  $M \in (0, N)$  represents the number of selected anchor postures, and the value 6 represents the motion feature. Our objective is to generate a plausible contiguous human motion sequence  $\hat{X}$  that exhibits coherent kinematic structures and smooth transitions.

#### 3.1 Preliminaries of Diffusion

Diffusion models are generative frameworks that capture data distributions by progressively injecting noise into the data (the forward process) and subsequently learning to reverse this process via denoising (the reverse process). In our work, conditions provided include the trajectory  $\tau$ , the sparse anchor postures  $X_s$ , and the timestep  $t$ , and our objective is to generate a complete motion sequence  $\hat{X}$ .

Starting with an initial sample  $X_0$  drawn from the motion data distribution, the forward process iteratively adds Gaussian noise along a fixed Markov chain of  $T$  steps until the sample is transformed into pure Gaussian noise, i.e.,  $X_T \sim \mathcal{N}(0, I)$ . This process is formally defined as follows:

$$q(X_t | X_{t-1}) = \mathcal{N}(X_t; \sqrt{\alpha_t} X_{t-1}, (1 - \alpha_t)I),$$

where  $\alpha_t \in (0, 1)$  denotes the predefined noise schedule,  $\mathcal{N}(\cdot)$  represents a Gaussian distribution, and  $I$  is the identity matrix.

The reverse process approximates the true posterior  $q(X_{t-1} | X_t)$  by learning to denoise the data using a neural network  $\epsilon_\theta$ . Notably, inspired by prior work [45], our model is designed to directly predict the motion sequence rather than the noise. Moreover, while the original DDPM sampling process requires a large number of timesteps (e.g.,  $T \approx 1000$ ) to produce high-quality samples, we accelerate sampling by employing DPM-Solver++, a high-order ODE solver tailored for diffusion models.

The reverse process is formulated as the following differential equation:

$$\frac{dX_t}{dt} = f(t)X_t + g(t)\epsilon_\theta(X_t, t, \tau, X_s),$$

where  $f(t)$  and  $g(t)$  are coefficients derived from the noise schedule, and the neural network  $\epsilon_\theta$  directly predicts the generated motion  $\hat{X}$ , conditioned on the trajectory  $\tau$ , the sparse anchor poses  $X_s$ , and the timestep  $t$ .

DPM-Solver++ resolves this equation using a semi-linear multi-step method, thereby significantly reducing the number of sampling

steps. The update rule is given by:

$$X_{t_{n+1}} = X_{t_n} + \Delta t \sum_{k=0}^K \gamma_k \epsilon_\theta^{(k)}(X_{t_{n-k}}, t_{n-k}, \tau, X_s),$$

where  $\Delta t$  is the adaptive step size,  $\gamma_k$  are the coefficients for the  $k$ -th order approximation, and  $\epsilon_\theta^{(k)}$  represents the  $k$ -th order derivative of the network prediction. This method enables high-quality sampling in as few as 20–30 steps, offering a substantial efficiency improvement over the original DDPM process.

#### 3.2 The structure of ProMoGen

Before formal training, the process begins by setting a specific temporal density  $f_n$  and interval elasticity  $f_s$ , then these two values are fed into the Filtering Module we designed to build the sparse anchor postures  $X_s$ . Next, the trajectory  $\tau$  and the sparse postures  $X_s$  are fed into the ProMoGen to predict the synthesized motion  $\hat{X}$ . We adopt Dit framework [34, 55], to develop fine-designed encoders and a refinement module to enhance motion synthesis. An overview of all components is presented below, also shown in the right panel of the Figure 2.

**3.2.1 Filtering Module.** In order to enable users to arbitrarily modify the insertion positions of postures, we introduce a Filtering Module (FM) that leverages a probabilistic algorithm during the training stage to imitate users' operations. This algorithm selects a set of anchor postures from a sequence of length  $N$  while satisfying two key constraints: (1) a fixed number of anchor poses, defined as the temporal density  $f_n$ , and (2) a minimum interval between any two selected anchor frames, termed as interval elasticity  $f_s$ . By uniformly sampling all potential valid combinations of anchor postures under these user-specified constraints, our design facilitates a flexible combination of conditions and enhances the system's adaptability, extremely extend the practical scale of training data.

The process is executed in three distinct steps: 1. Virtual sampling point selection, 2. Interval increment calculation, and 3. Anchor position mapping, which collectively use the parameters  $f_n$  and  $f_s$ .

Initially,  $f_n$  virtual positions are randomly selected from the set:

$$\mathcal{P} = \{p_1, p_2, \dots, p_{f_n}\} \subset \{1, 2, \dots, T_{\text{total}}\}, \quad |\mathcal{P}| = f_n,$$

where the total number of virtual sampling points is given by  $T_{\text{total}} = R + f_n$ . Here,

$$R = N - [f_n + (f_n - 1)f_s]$$

represents the difference between the total sequence length  $N$  and the minimal length required by the rigid constraint. The value  $R$  quantifies the available extra intervals, which are distributed as the elastic interval increments  $\{\delta_i\}_{i=0}^{f_n}$  under the constraint:  $\sum_{i=0}^{f_n} \delta_i = R$ . These elastic interval increments correspond to the additional spacing beyond the predefined minimum  $f_s$  between consecutive anchors, and are defined as follows:

$$\begin{cases} \delta_0 = p_1 - 1, \\ \delta_i = p_{i+1} - p_i - 1, & \text{for } 1 \leq i < f_n, \\ \delta_{f_n-1} = T_{\text{total}} - p_{f_n}. \end{cases}$$



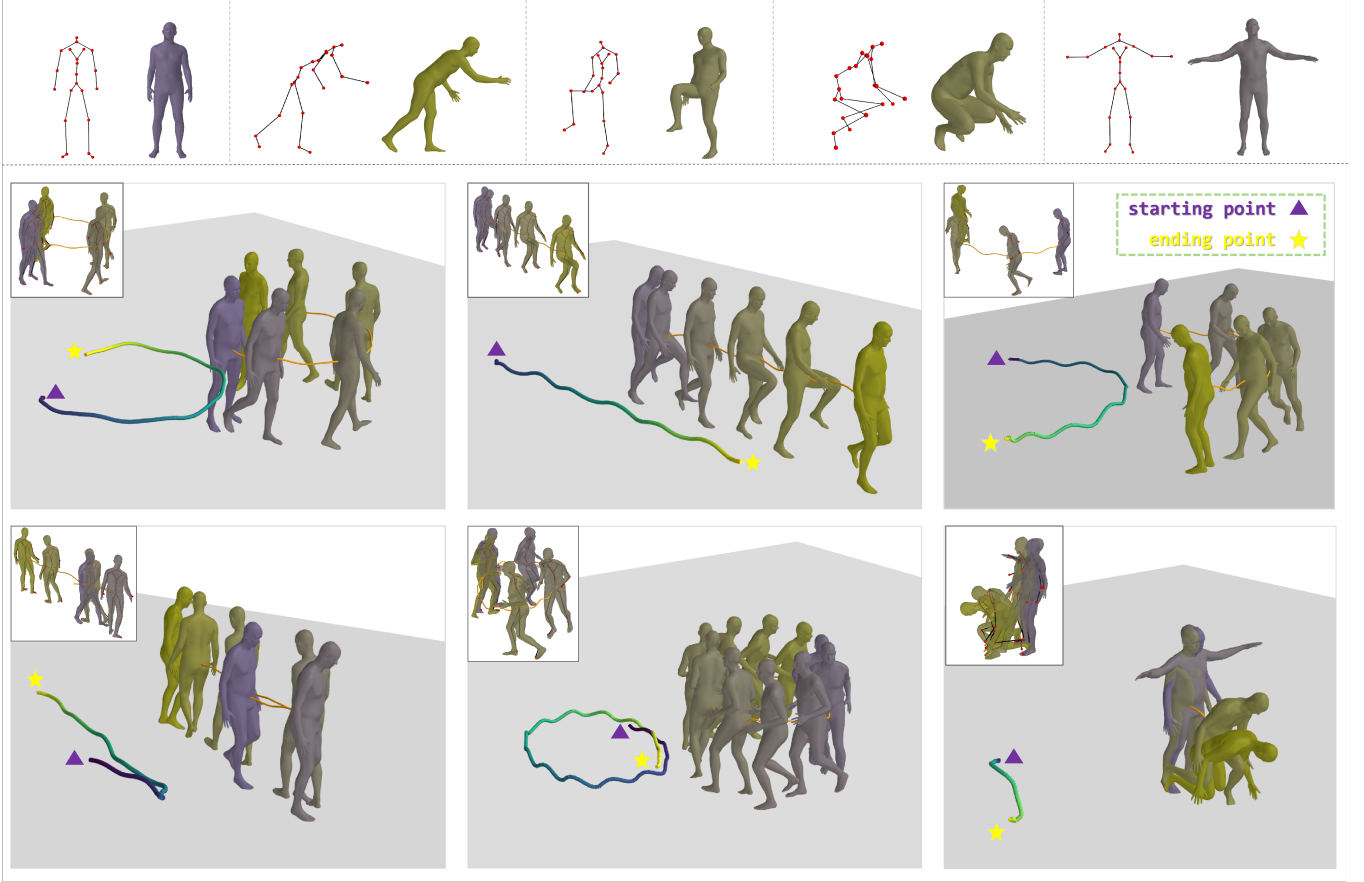


**Figure 4:** This figure illustrates the trajectory-based, sparse pose-guided motion generation process of our ProMoGen. In the top row, the reconstructed anchor motion (displayed as a mesh on the right) is compared with the control pose (depicted as a skeleton on the left), demonstrating a high degree of correspondence. In each of the subsequent sub-figures, the primary visualization represents the reconstructed motion, while the lines on the left indicate the trajectory. Color coding is applied such that both the character and the trajectory transition from purple (starting point) to yellow (ending point). The upper left corner of each sub-figure provides the guidance of sparse poses. All visualizations in this figure are derived from inferences made under the condition that the number of sparse anchor poses  $f_n$  is fixed at five.

Finally, the anchor positions  $X_s = \{x_s^1, x_s^2, \dots, x_s^{f_n}\}$  are determined by the mapping:

$$\begin{cases} x_1 = \delta_0 + 1, \\ x_j = x_{j-1} + f_s + \delta_{j-1} + 1, \quad \forall j > 1. \end{cases}$$

This recurrence can be expressed in closed form as:

$$x_j = j + (j-1)f_s + \sum_{i=0}^{j-1} \delta_i.$$

Regarding the properties of the algorithm, the interval between any two adjacent anchors is given by:

$$x_k - x_{k-1} = f_s + \delta_{k-1} + 1,$$

which guarantees that:

$$x_k - x_{k-1} \geq f_s + 1 > f_s.$$

Thus, the design robustly ensures that the minimum spacing condition is strictly maintained. During the training stage, the FM is both

computationally efficient and mathematically rigorous to imitate the user-specific sparse anchor postures constraints.

**3.2.2 Network Design.** The proposed network is a hierarchical transformer-based architecture designed conditioned human motion synthesis with the control of trajectory and sparse anchor motions guidance. It comprises five core modules:

1). Trajectory Encoder  $\mathcal{E}_\tau$ : Maps the raw trajectory  $\tau$  into a latent space. 2). Anchor Motion Encoder  $\mathcal{E}_k$ : Encodes the sparse postures constraints into contextual features. 3). Initial Motion Generator  $\mathcal{G}$ : Synthesizes coarse motion priors conditioned solely on trajectory features, as defined by:

$$M_{init} = \mathcal{G}(x_t, \mathcal{E}_k(X_s)) \in \mathbb{R}^{N \times 512}.$$

4). Refinement Module  $\mathcal{R}$ : Jointly refines the motion priors by integrating both trajectory and anchor pose features:

$$M_{refined} = \mathcal{R}(M_{init} \oplus \mathcal{E}_k(X_s) \oplus \mathcal{E}_\tau(\tau)),$$

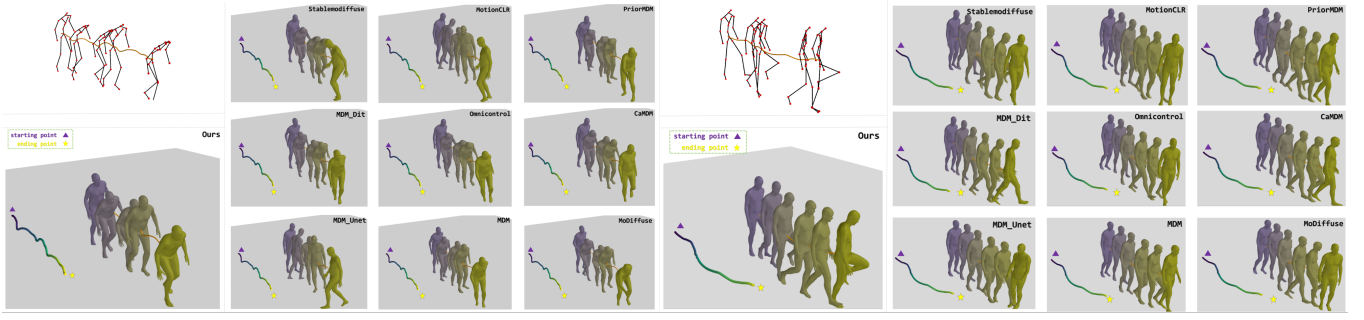


**Figure 5:** The figure illustrates the comparative generation effects of various modules. Under identical trajectory and anchor postures, the motions synthesized by our model are notably smoother and exhibit richer dynamic variations. Furthermore, the generated motions of ProMoGen most accurately adhere to the sparse poses guidance, highlighting the superior performance of our approach.

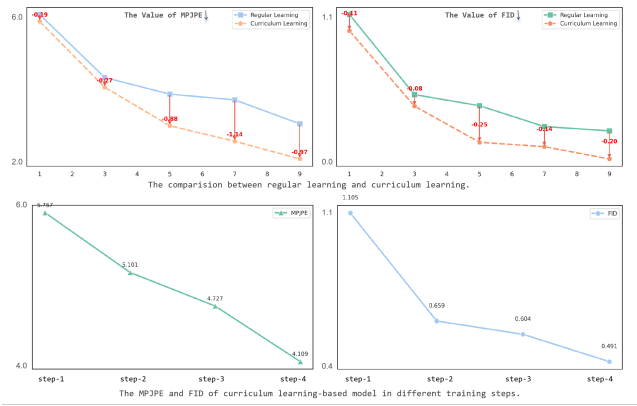


**Figure 6:** The two figures above display the changing of FID and MPJPE metrics, comparing regular training with curriculum learning. The curriculum learning yields significant improvements in model performance across varying numbers of anchor poses. The subfigures below further demonstrate that as the curriculum learning stages progress, model performance progressively enhances.

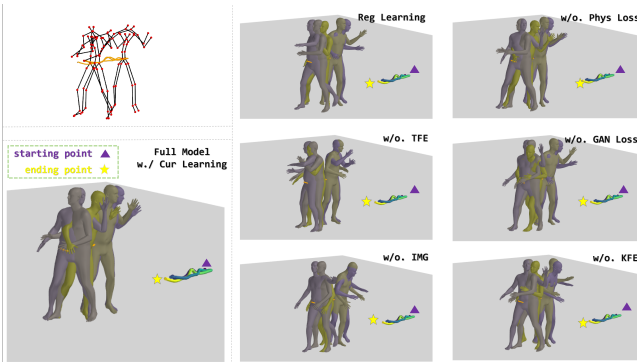


**Figure 7:** The figure presents a series of ablation experiments that examine the effects of various modules and loss functions on the overall performance of the model.

where  $\oplus$  denotes feature concatenation. 5). Decoder  $\mathcal{D}$ : Projects the refined features into full kinematic motion sequences.

All modules adopt Dit(Diffusion Transformer) architecture for effective spatial-temporal modeling. This architecture facilitates motion distribution learning of trajectory-aligned motions while ensuring the anchor poses constraints, and have a good Spatial-Temporal learning and prediction ability.

**3.2.3 The optimization target.** The overall loss function of our framework is composed of several components designed to enforce both global consistency and local accuracy in the synthesized motion. Specifically, the loss terms include: 1) $L_2$  Loss: Directly computes the Euclidean difference between the ground truth motion  $X$  and the synthesized motion  $\hat{X}$ ; 2)Anchor Motion Loss  $\mathcal{L}_{anchor}$ : Specifically penalizes discrepancies in the postures at selected anchor positions; 3)GAN Loss  $\mathcal{L}_G$ : Enhances the naturalness and global coherence of the motion by leveraging adversarial training; 4)Joint Loss  $\mathcal{L}_J$ : Ensures local accuracy by enforcing precise predictions for individual joints; 5)Physical Constraints  $\mathcal{L}_P$ : Imposes realistic motion through constraints such as foot slip reduction, body float minimization, and ground penetration prevention.

The total loss is thus formulated as:

$$\mathcal{L}_{total} = \lambda_1 \mathcal{L}_2 + \lambda_2 \mathcal{L}_{anchor} + \lambda_3 \mathcal{L}_J + \lambda_4 \mathcal{L}_G + \lambda_5 \mathcal{L}_P.$$

During training, the weighting factors are set as  $\lambda_1 = \lambda_2 = \lambda_3 = 1.0$  and  $\lambda_4 = \lambda_5 = 0.1$ .

### 3.3 Sparse Anchor Posture Curriculum Learning

Under a total of  $E_{total}$  training epochs, the process is segmented into  $E_{stage}$  stages, each corresponding to a anchor sampling interval  $[K_{min}^{(s)}, K_{max}]$ . Here,  $s \in \{1, \dots, E_{stage}\}$  denotes the stage index, and  $K_{max}$  is fixed at 30, as we posit that incorporating more than 30 anchor motions will introduce redundant, homogeneous information. The initial stage employs the configuration with  $K_{min}^{(1)} = 20$ , and subsequent stages progressively reduce the minimum number of anchor postures, culminating in the final stage where a single action ( $K_{min}^{(s)} = 1$ ) is permitted.

Method	MPJPE ↓		JS ↓		Diversity →		DM ↑		K-MPJPE ↓		FID ↓	
	DS-1	DS-2	DS-1	DS-2	DS-1	DS-2	DS-1	DS-2	DS-1	DS-2	DS-1	DS-2
MDM	5.510 ±0.103	6.685 ±0.088	<u>0.020</u> ±0.001	0.039 ±0.001	4.455 ±0.020	4.744 ±0.015	<u>4.011</u> ±0.029	1.845 ±0.049	5.488 ±0.102	6.671 ±0.092	1.093 ±0.030	1.119 ±0.039
CAMDm	5.452 ±0.068	6.607 ±0.065	<b>0.019</b> ±0.001	0.035 ±0.001	4.476 ±0.011	4.691 ±0.014	3.978 ±0.031	1.981 ±0.036	5.435 ±0.069	6.492 ±0.061	1.071 ±0.027	1.122 ±0.035
MotionDiffuse	5.646 ±0.092	6.531 ±0.089	0.066 ±0.001	0.038 ±0.001	4.504 ±0.014	4.735 ±0.011	3.249 ±0.037	2.004 ±0.031	5.631 ±0.090	6.495 ±0.086	0.735 ±0.022	0.804 ±0.024
MotionCLR	14.676 ±0.164	14.187 ±0.099	0.035 ±0.001	0.033 ±0.001	4.410 ±0.011	4.646 ±0.009	2.678 ±0.051	1.471 ±0.049	14.515 ±0.156	13.909 ±0.101	11.811 ±0.076	8.703 ±0.115
PriorMDM	6.403 ±0.101	9.225 ±0.094	0.021 ±0.001	0.041 ±0.001	4.432 ±0.016	4.725 ±0.009	3.952 ±0.031	1.680 ±0.043	6.394 ±0.101	9.232 ±0.098	1.386 ±0.045	1.729 ±0.051
StableMoFusion	6.112 ±0.104	5.768 ±0.070	0.033 ±0.001	<u>0.032</u> ±0.001	4.517 ±0.013	<u>4.754</u> ±0.014	3.813 ±0.028	<u>2.158</u> ±0.038	6.063 ±0.102	5.699 ±0.071	0.420 ±0.013	0.512 ±0.019
GMD-unet	14.633 ±0.131	14.535 ±0.088	0.042 ±0.001	0.037 ±0.001	4.486 ±0.012	4.640 ±0.007	2.562 ±0.050	1.413 ±0.033	14.524 ±0.133	14.529 ±0.088	12.029 ±0.047	8.896 ±0.094
GMD-dit	5.763 ±0.076	6.652 ±0.103	0.033 ±0.001	0.036 ±0.001	<u>4.521</u> ±0.018	4.736 ±0.009	3.777 ±0.030	1.922 ±0.048	5.734 ±0.076	6.658 ±0.102	0.887 ±0.029	0.916 ±0.034
OmniControl	5.647 ±0.058	6.464 ±0.097	0.027 ±0.001	0.035 ±0.001	4.478 ±0.015	4.743 ±0.011	3.960 ±0.034	1.941 ±0.049	5.627 ±0.060	6.450 ±0.101	0.943 ±0.018	0.885 ±0.022
Ours-v1	4.189 ±0.077	4.289 ±0.055	0.032 ±0.002	0.073 ±0.001	4.516 ±0.015	4.732 ±0.013	3.866 ±0.055	1.806 ±0.050	<u>3.754</u> ±0.061	<u>4.006</u> ±0.055	<u>0.418</u> ±0.012	<u>0.438</u> ±0.020
Ours-v2	3.257 ±0.062	3.654 ±0.049	0.030 ±0.001	<b>0.032</b> ±0.001	<b>4.531</b> ±0.015	<b>4.768</b> ±0.011	<b>4.278</b> ±0.041	<b>2.656</b> ±0.064	<b>3.247</b> ±0.062	<b>3.648</b> ±0.046	<b>0.279</b> ±0.012	<b>0.412</b> ±0.017

**Table 1: Performance comparison of various methods across multiple metrics on HumanML3D [16](DS-1) and CombatMotion [56](DS-2) respectively. The best results are in bold, and the second best results are underlined. ↓ means the lower is better while ↑ means the higher is better. → represents the closer to the value of Real is better.**

During each stage  $k$ , the temporal density  $f_n^k$  is constructed by randomly sampling  $f_n^k \in [K_{\min}^{(s)}, K_{\max}]$ , the interval elasticity  $f_s^k \in [4, \lfloor \frac{N}{f_n^k} \rfloor]$ , which is used to set the minimum interval between any two anchor motions, the  $f_s^k$  will not exceed the maximum value  $\lfloor \frac{N}{f_n^k} \rfloor$ . By gradually transitioning from dense ( $K_{\min} = 20$ ) to sparse ( $K_{\min} = 1$ ) configurations, the model incrementally adapts to the anchor-missing generation task, thereby mitigating the risk of mode collapse that can arise from direct sparse training. The whole process is shown in Algorithm 1

#### Algorithm 1 Sparse Anchor Progressive Curriculum Learning

**Require:** Total epochs  $E_{\text{total}}$ , predefined curriculum learning stages  $E_{\text{stage}}$ , maximum anchor poses  $K_{\max} = 30$   
**Ensure:** Trained diffusion model

- 1: Initialize model parameters  $\theta$
- 2: **for**  $s = 1$  to  $E_{\text{stage}}$  **do**
- 3:   **Compute minimum anchor poses:**
- 4:   **if**  $s = 1$  **then**
- 5:      $K_{\min}^{(s)} \leftarrow 20$  ▷ Initial dense phase
- 6:   **else if**  $s = E_{\text{stage}}$  **then**
- 7:      $K_{\min}^{(s)} \leftarrow 1$  ▷ Final sparse phase
- 8:   **else**
- 9:      $K_{\min}^{(s)} \leftarrow \left\lfloor 20 - \frac{19(s-1)}{E_{\text{stage}}-1} \right\rfloor$  ▷ Linear interpolation
- 10:   **end if**
- 11:   **Stage epochs:**  $E_{\text{stage\_epochs}} \leftarrow E_{\text{total}}/E_{\text{stage}}$
- 12:   **for**  $e = 1$  to  $E_{\text{stage\_epochs}}$  **do**
- 13:     **Set temporal density and interval elasticity:**  $f_n^k \sim \mathcal{U}(K_{\min}^{(s)}, K_{\max})$ ,  $f_s^k \sim \mathcal{U}(4, \lfloor \frac{N}{f_n^k} \rfloor)$
- 14:     **Build Anchor conditions:**  $X_s \leftarrow FM(f_n^k, f_s^k) \leftarrow f_n^k, f_s^k$
- 15:     **Train model:**  $\theta \leftarrow \theta - \nabla_{\theta} \mathcal{L}_{\text{total}}(x_t, t, \tau, X_s)$  ▷ Update via  $\mathcal{L}_{\text{total}}$
- 16:   **end for**
- 17: **end for**
- 18: **return**  $\theta$

## 4 Experiments

**Datasets:** We evaluate our method on two datasets. For quantitative comparisons between our framework and other approaches, we

employ the HumanML3D [16] dataset, which consists of 14,646 motion sequences, and the CombatMotion [56] dataset, which includes 14,883 motion sequences. To assess the impact of the curriculum learning strategy, we perform comparisons using the HumanML3D dataset. Additionally, ablation studies investigating the effects of various components are conducted on the HumanML3D dataset.

**Evaluation Metrics** Our framework is assessed using several metrics: 1. MPJPE (Mean Per Joint Position Error): Computes the Euclidean distance between corresponding joints of the generated and ground truth motions. 2. JS (Joint Smoothness): Evaluates the smoothness of transitions between adjacent frames. 3. Diversity: Measures the variance across generated motions to assess variety. 4. Directional Consistency: Quantifies the similarity between the predicted motion direction and the actual motion trajectory. 5. K-MPJPE: Assesses the Euclidean distance specifically at anchor positions. 6. FID (Fréchet Inception Distance) [18]: Evaluates the distributional gap between the generated and real motion data.

**Implement Details:** Because this work is to synthesize human motion by simultaneously conditioning on trajectory data and sparse anchor postures. In contrast, prior methods predominantly rely on text-based input. For fair comparison and to demonstrate the efficacy of our framework, we reconstruct these baseline methods by removing their text encoders and substituting them with two linear layers that serve as trajectory and sparse posture encoders, respectively. In our evaluations, this same variant is denoted as Ours-v1, while the full model incorporating all proposed components is as Ours-v2.

In order to fairly compare our model with other models, motions from all datasets have been retargeted into one skeleton following HumanML3D format with 20 fps, where the number of joint  $\mathcal{J}$  is 22. The learning rate is set to be 0.0001. The  $E_{\text{total}}$  is set to be 100. The  $E_{\text{stage}}$  is set as 4. The timesteps are set to 1000 for training and 25 for inference. Our models are trained on one RTX 4070Ti with each batch of 32.

### 4.1 Quantitative and Qualitative Results

As shown in Figure 4, our framework exhibits robust capabilities in generating motion that is both trajectory-aligned and anchor poses aligned, resulting in the stylistic and dynamic consistent motion synthesis, thereby demonstrating its versatility and performance. Table 1 illustrates that our ProMoGen variant utilizing a simple linear encoder (Ours-v1) already outperforms competing methods on most evaluation metrics, while the full ProMoGen model

Method	A-Num	MPJPE ↓	JS ↓	Diversity →	DM ↑	K-MPJPE ↓	FID ↓
Ours(Regular) vs. Ours(Curriculum)	9-Reg	3.101 ±0.046	0.032 ±0.001	4.504 ±0.016	4.310 ±0.025	3.099 ±0.047	0.319 ±0.010
	9-Cur	<b>2.130</b> ±0.029	<b>0.031</b> ±0.001	<b>4.515</b> ±0.012	<b>4.506</b> ±0.036	<b>2.127</b> ±0.028	<b>0.124</b> ±0.005
	7-Reg	3.762 ±0.037	0.031 ±0.001	4.505 ±0.011	4.258 ±0.027	3.234 ±0.036	0.349 ±0.013
	7-Cur	<b>2.618</b> ±0.051	<b>0.030</b> ±0.001	<b>4.511</b> ±0.015	<b>4.403</b> ±0.029	<b>2.624</b> ±0.052	<b>0.209</b> ±0.012
	5-Reg	3.922 ±0.061	0.031 ±0.001	4.493 ±0.017	4.228 ±0.043	3.911 ±0.061	0.494 ±0.019
	5-Cur	<b>3.047</b> ±0.040	<b>0.030</b> ±0.001	<b>4.510</b> ±0.012	<b>4.285</b> ±0.032	<b>3.003</b> ±0.039	<b>0.240</b> ±0.010
	3-Reg	4.379 ±0.056	0.030 ±0.000	4.483 ±0.016	4.166 ±0.024	4.341 ±0.057	0.571 ±0.015
	3-Cur	<b>4.109</b> ±0.070	<b>0.029</b> ±0.001	<b>4.519</b> ±0.014	<b>4.212</b> ±0.025	<b>4.107</b> ±0.069	<b>0.491</b> ±0.017
	1-Reg	6.119 ±0.095	0.029 ±0.001	4.482 ±0.019	<b>4.073</b> ±0.034	6.077 ±0.092	1.127 ±0.033
	1-Cur	<b>5.929</b> ±0.084	<b>0.028</b> ±0.002	<b>4.514</b> ±0.011	4.055 ±0.034	<b>5.915</b> ±0.086	<b>1.014</b> ±0.023

**Table 2: The performance comparison of ProMoGen under both regular and curriculum learning paradigms-using varying numbers of anchor guidance along the same trajectory on the HumanML3D [16] dataset-is presented, with the best results highlighted in bold.**

Method	Components	MPJPE ↓	JS ↓	Diversity →	DM ↑	K-MPJPE ↓	FID ↓
Ours Full Model	w/o. IMG	3.670 ±0.079	0.029 ±0.001	4.499 ±0.019	4.243 ±0.030	3.672 ±0.082	0.419 ±0.016
	w/o. TFE	7.202 ±0.102	<b>0.025</b> ±0.001	4.452 ±0.011	4.009 ±0.044	7.193 ±0.103	1.596 ±0.041
	w/o. AME	3.531 ±0.066	0.032 ±0.001	4.499 ±0.017	4.264 ±0.031	3.529 ±0.065	0.371 ±0.013
	w/o. GAN loss	3.326 ±0.054	0.031 ±0.001	4.495 ±0.016	4.276 ±0.036	3.321 ±0.055	0.330 ±0.014
	w/o. Phys loss	3.251 ±0.046	0.030 ±0.001	4.510 ±0.015	4.265 ±0.034	3.221 ±0.045	0.296 ±0.015
	w/. Reg Learning	3.257 ±0.062	0.030 ±0.001	<b>4.531</b> ±0.015	4.278 ±0.041	3.247 ±0.062	0.279 ±0.012
	w/. Cur Learning	<b>3.047</b> ±0.040	0.030 ±0.001	4.510 ±0.012	<b>4.285</b> ±0.032	<b>3.003</b> ±0.039	<b>0.240</b> ±0.010

**Table 3: Ablation studies for our model on HumanML3D [16] dataset, the best results are in bold.**

(Ours-v2) further make progress on these metrics. All experiments reported in Table 1 were conducted under standard training conditions, thereby underscoring the superiority of our structure. The reason is our ProMoGen decouples trajectory and motion by assigning distinct encoders to each, thereby enhancing the understanding and mapping of their specific conditional features. In addition, our initial motion generator leverages trajectory information to produce a coarse global motion, establishing a rough alignment between trajectory and motion features, where the coarse motion is then progressively refined and focus exclusively on local details by the refinement module. This approach still embodies an easy-to-hard learning paradigm, ultimately leading to improved performance.

Figure 5 presents the comparative results, while Figure 3 illustrates the FID scatter plot for all methods listed in Table 1. To ensure the visual effect, the values for all models have been normalized to a uniform scale. Notably, our ProMoGen model is positioned in the upper right quadrant of the scatter plot, demonstrating its superior performance on both the HumanML3D [16] and Combat-Motion [56] datasets.

## 4.2 Curriculum Learning Studies

Table 2 demonstrates the effectiveness of our curriculum training strategy. The "A-Num" denotes the number of anchor postures used as conditioning inputs. As observed in Table 2, increasing the number of anchor poses generally leads to improved metric values, which is an intuitive outcome. Moreover, curriculum training yields significant improvements across nearly all metrics for all configurations. The upper section of Figure 6 provides a detailed comparison between the two training paradigms under identical conditions, while the lower section illustrates the reduction in both MPJPE and FID when employing a progressively easy-to-hard training approach.

## 4.3 Ablation Studies

In this section, we conduct a series of ablation experiments to rigorously evaluate the contributions of individual components within our framework, as observed in Table 3. Specifically, we sequentially remove the Initial Motion Generator (IMG), the Trajectory Feature Encoder (TFE), the Anchor Motion Encoder (AME) and two losses in separate experimental settings to assess their impact on overall performance.

The results demonstrate that the TFE plays a pivotal role in enhancing the model's capability, followed by IMG and AME, moreover, GAN and Phys Loss can further improve the precision of the results. Figure 7 provides visualizations under various ablation conditions, clearly illustrating that our complete model reconstructs postures with high fidelity. These findings substantiate the critical contributions of each module and validate the robustness of our design.

## 5 Conclusion

Building on our proposed Trajectory-Sparse Postures-Motion task, we have developed the ProMoGen framework to synthesize human motion with high fidelity and flexibility. To accelerate the inference process, we have incorporated DPM-Solver++, a high-order ODE solver tailored for diffusion models. During the training, we design the Filtering Module to sample sparse anchor motions in uniformly probabilistic sampling from the predefined  $(f_n, f_s)$ , to extend the practical training scale and imitate the user-specific choice. Then we introduce a novel curriculum learning strategy SAP-CL that follows an easy-to-hard paradigm, which substantially enhances the quality of the generated motion. The extensive comparison experiments and ablations demonstrate the ability of ProMoGen and the effectiveness of SAP-CL. More details and results are shown in the **Appendix**.



In all, Our framework is capable of seamlessly fusing arbitrary motion cues by conditioning on a specified trajectory, thereby achieving smooth and highly flexible motion generation. Overall, the ProMoGen framework demonstrates superior versatility, performance, and efficiency when compared to existing state-of-the-art methods, underscoring its potential for advancing the field of human motion synthesis.

## References

- [1] Nikos Athanasiou, Alpár Cseke, Markos Diomataris, Michael J Black, and Gül Varol. 2024. MotionFix: Text-driven 3d human motion editing. In *SIGGRAPH Asia 2024 Conference Papers*. 1–11.
- [2] Nikos Athanasiou, Mathis Petrovich, Michael J Black, and Gül Varol. 2023. SINC: Spatial composition of 3D human motions for simultaneous action generation. In *Proceedings of the IEEE/CVF International Conference on Computer Vision*. 9984–9995.
- [3] Yoshua Bengio, Jérôme Louradour, Ronan Collobert, and Jason Weston. 2009. Curriculum learning. In *Proceedings of the 26th annual international conference on machine learning*. 41–48.
- [4] Ling-Hao Chen, Shunlin Lu, Wenxun Dai, Zhiyang Dou, Xuan Ju, Jingbo Wang, Taku Komura, and Lei Zhang. 2024. Pay Attention and Move Better: Harnessing Attention for Interactive Motion Generation and Training-free Editing. *arXiv preprint arXiv:2410.18977* (2024).
- [5] Rui Chen, Mingyi Shi, Shaoli Huang, Ping Tan, Taku Komura, and Xuelin Chen. 2024. Taming diffusion probabilistic models for character control. In *ACM SIGGRAPH 2024 Conference Papers*. 1–10.
- [6] Kiran Chhatre, Nikos Athanasiou, Giorgio Becherini, Christopher Peters, Michael J Black, Timo Bolkart, et al. 2024. Emotional speech-driven 3d body animation via disentangled latent diffusion. In *Proceedings of the IEEE/CVF Conference on Computer Vision and Pattern Recognition*. 1942–1953.
- [7] Seunggeun Chi, Hyung-gun Chi, Hengbo Ma, Nakul Agarwal, Faizan Siddiqui, Karthik Ramani, and Kwonjoon Lee. 2024. M2d2m: Multi-motion generation from text with discrete diffusion models. In *European Conference on Computer Vision*. Springer, 18–36.
- [8] Yuchen Chu and Zeshi Yang. 2024. Real-time Diverse Motion In-betweening with Space-time Control. In *Proceedings of the 17th ACM SIGGRAPH Conference on Motion, Interaction, and Games*. 1–8.
- [9] Setareh Cohan, Guy Tevet, Daniele Reda, Xue Bin Peng, and Michiel van de Panne. 2024. Flexible motion in-betweening with diffusion models. In *ACM SIGGRAPH 2024 Conference Papers*. 1–9.
- [10] Peishan Cong, Ziyi Wang, Zhiyang Dou, Yiming Ren, Wei Yin, Kai Cheng, Yujing Sun, Xiaoxiao Long, Xinge Zhu, and Yuexin Ma. 2024. Laserhuman: language-guided scene-aware human motion generation in free environment. *arXiv preprint arXiv:2403.13307* (2024).
- [11] Rishabh Dabral, Muhammad Hamza Mughal, Vladislav Golyanik, and Christian Theobalt. 2023. Mofusion: A framework for denoising-diffusion-based motion synthesis. In *Proceedings of the IEEE/CVF conference on computer vision and pattern recognition*. 9760–9770.
- [12] Minyue Dai, Jingbo Wang, Ke Fan, Bin Ji, Haoyu Zhao, Junting Dong, and Bo Dai. 2025. Towards Synthesized and Editable Motion In-Betweening Through Part-Wise Phase Representation. *arXiv:2503.08180 [cs.CV]* <https://arxiv.org/abs/2503.08180>
- [13] Wenxun Dai, Ling-Hao Chen, Jingbo Wang, Jinpeng Liu, Bo Dai, and Yansong Tang. 2024. Motionlcm: Real-time controllable motion generation via latent consistency model. In *European Conference on Computer Vision*. Springer, 390–408.
- [14] Canxuan Gang and Yiran Wang. 2025. Human Motion Prediction, Reconstruction, and Generation. *arXiv preprint arXiv:2502.15956* (2025).
- [15] Chuan Guo, Yuxuan Mu, Muhammad Gohar Javed, Sen Wang, and Li Cheng. 2024. Momask: Generative masked modeling of 3d human motions. In *Proceedings of the IEEE/CVF Conference on Computer Vision and Pattern Recognition*. 1900–1910.
- [16] Chuan Guo, Shihao Zou, Xinxin Zuo, Sen Wang, Wei Ji, Xingyu Li, and Li Cheng. 2022. Generating Diverse and Natural 3D Human Motions From Text. In *Proceedings of the IEEE/CVF Conference on Computer Vision and Pattern Recognition (CVPR)*. 5152–5161.
- [17] Ziyang Guo, Zeyu Hu, Na Zhao, and De Wen Soh. 2025. MotionLab: Unified Human Motion Generation and Editing via the Motion-Condition-Motion Paradigm. *arXiv preprint arXiv:2502.02358* (2025).
- [18] Martin Heusel, Hubert Ramsauer, Thomas Unterthiner, Bernhard Nessler, and Sepp Hochreiter. 2017. Gans trained by a two time-scale update rule converge to a local nash equilibrium. *Advances in neural information processing systems* 30 (2017).
- [19] Jonathan Ho, Ajay Jain, and Pieter Abbeel. 2020. Denoising diffusion probabilistic models. *Advances in neural information processing systems* 33 (2020), 6840–6851.
- [20] Jonathan Ho, Tim Salimans, Alexey Gritsenko, William Chan, Mohammad Norouzi, and David J Fleet. 2022. Video diffusion models. *Advances in Neural Information Processing Systems* 35 (2022), 8633–8646.
- [21] Yiheng Huang, Hui Yang, Chuanchen Luo, Yuxi Wang, Shibiao Xu, Zhaoxiang Zhang, Man Zhang, and Junran Peng. 2024. Stablefusion: Towards robust and efficient diffusion-based motion generation framework. In *Proceedings of the 32nd ACM International Conference on Multimedia*. 224–232.
- [22] Zhongyu Jiang, Wenhao Chai, Zhuoran Zhou, Cheng-Yen Yang, Hsiang-Wei Huang, and Jenq-Neng Hwang. 2025. PackDiT: Joint Human Motion and Text Generation via Mutual Prompting. *arXiv preprint arXiv:2501.16551* (2025).
- [23] Gaurav Kamath, Sebastian Schuster, Sowmya Vajjala, and Siva Reddy. 2024. Scope ambiguities in large language models. *Transactions of the Association for Computational Linguistics* 12 (2024), 738–754.
- [24] Kacper Kania, Marek Kowalski, and Tomasz Trzcinski. 2021. Trajevae: Controllable human motion generation from trajectories. *arXiv preprint arXiv:2104.00351* (2021).
- [25] Korrawe Karunratanakul, Konpat Preechakul, Supasorn Suwajanakorn, and Siyu Tang. 2023. Guided motion diffusion for controllable human motion synthesis. In *Proceedings of the IEEE/CVF International Conference on Computer Vision*. 2151–2162.
- [26] Aryan Keluskar, Amrita Bhattacharjee, and Huan Liu. 2024. Do LLMs Understand Ambiguity in Text? A Case Study in Open-world Question Answering. In *2024 IEEE International Conference on Big Data (BigData)*. IEEE, 7485–7490.
- [27] Huiyong Joon Kim, Youna Kim, Cheonbok Park, Junyeob Kim, Choonghyun Park, Kang Min Yoo, Sang-goo Lee, and Taeuk Kim. 2024. Aligning language models to explicitly handle ambiguity. *arXiv preprint arXiv:2404.11972* (2024).
- [28] Jihoon Kim, Taehyun Byun, Seungyoun Shin, Jungdam Won, and Sungjoon Choi. 2022. Conditional motion in-betweening. *Pattern Recognition* 132 (2022), 108894.
- [29] Jisu Kim and Juhwan Lee. 2024. Strategic Data Ordering: Enhancing Large Language Model Performance through Curriculum Learning. *arXiv preprint arXiv:2405.07490* (2024).
- [30] So Young Lee, Russell Scheinberg, Amber Shore, and Ameeta Agrawal. 2025. Multilingual Relative Clause Attachment Ambiguity Resolution in Large Language Models. *arXiv preprint arXiv:2503.02971* (2025).
- [31] Fenglin Liu, Shen Ge, Yuexian Zou, and Xian Wu. 2022. Competence-based multimodal curriculum learning for medical report generation. *arXiv preprint arXiv:2206.14579* (2022).
- [32] Shunlin Lu, Ling-Hao Chen, Ailing Zeng, Jing Lin, Ruimao Zhang, Lei Zhang, and Heung-Yeung Shum. 2023. Humantomato: Text-aligned whole-body motion generation. *arXiv preprint arXiv:2310.12978* (2023).
- [33] Sihan Ma, Qiong Cao, Jing Zhang, and Dacheng Tao. 2024. Contact-aware human motion generation from textual descriptions. *arXiv preprint arXiv:2403.15709* (2024).
- [34] Xin Ma, Yaohui Wang, Gengyun Jia, Xinyuan Chen, Ziwei Liu, Yuan-Fang Li, Cunjian Chen, and Yu Qiao. 2024. Latte: Latent diffusion transformer for video generation. *arXiv preprint arXiv:2401.03048* (2024).
- [35] Binyamin Manela and Armin Biess. 2022. Curriculum learning with hindsight experience replay for sequential object manipulation tasks. *Neural Networks* 145 (2022), 260–270.
- [36] Muhammad A Muttatqien, Ayanori Yoroza, and Akihisa Ohya. 2024. Mobile Robots through Task-Based Human Instructions using Incremental Curriculum Learning. In *2024 IEEE International Conference on Cybernetics and Intelligent Systems (CIS) and IEEE International Conference on Robotics, Automation and Mechatronics (RAM)*. IEEE, 232–237.
- [37] William Peebles and Saining Xie. 2023. Scalable diffusion models with transformers. In *Proceedings of the IEEE/CVF international conference on computer vision*. 4195–4205.
- [38] Mathis Petrovich, Michael J Black, and Gül Varol. 2022. Temos: Generating diverse human motions from textual descriptions. In *European Conference on Computer Vision*. Springer, 480–497.
- [39] Haoxuan Qu, Ziyang Guo, and Jun Liu. 2024. GPT-Connect: Interaction between Text-Driven Human Motion Generator and 3D Scenes in a Training-free Manner. *arXiv preprint arXiv:2403.14947* (2024).
- [40] Yonatan Shafir, Guy Tevet, Roy Kapon, and Amit H Bermano. 2023. Human motion diffusion as a generative prior. *arXiv preprint arXiv:2303.01418* (2023).
- [41] Mengyi Shan, Lu Dong, Yutao Han, Yuan Yao, Tao Liu, Ifeoma Nwogu, Guo-Jun Qi, and Mitch Hill. 2024. Towards open domain text-driven synthesis of multi-person motions. In *European Conference on Computer Vision*. Springer, 67–86.
- [42] Jiaming Song, Chenlin Meng, and Stefano Ermon. 2020. Denoising diffusion implicit models. *arXiv preprint arXiv:2010.02502* (2020).
- [43] Petru Soviany, Radu Tudor Ionescu, Paolo Rota, and Nicu Sebe. 2021. Curriculum self-paced learning for cross-domain object detection. *Computer Vision and Image Understanding* 204 (2021), 103166.
- [44] Guy Tevet, Brian Gordon, Amir Hertz, Amit H Bermano, and Daniel Cohen-Or. 2022. Motionclip: Exposing human motion generation to clip space. In *European Conference on Computer Vision*. Springer, 358–374.
- [45] Guy Tevet, Sigal Raab, Brian Gordon, Yonatan Shafir, Daniel Cohen-Or, and Amit H Bermano. 2022. Human motion diffusion model. *arXiv preprint*

- arXiv:2209.14916* (2022).
- [46] Ashish Vaswani, Noam Shazeer, Niki Parmar, Jakob Uszkoreit, Llion Jones, Aidan N Gomez, Łukasz Kaiser, and Illia Polosukhin. 2017. Attention is all you need. *Advances in neural information processing systems* 30 (2017).
  - [47] Weilin Wan, Zhiyang Dou, Taku Komura, Wenping Wang, Dinesh Jayaraman, and Lingjie Liu. 2024. Tlcontrol: Trajectory and language control for human motion synthesis. In *European Conference on Computer Vision*. Springer, 37–54.
  - [48] Congyi Wang. 2023. T2m-hifigt: generating high quality human motion from textual descriptions with residual discrete representations. *arXiv preprint arXiv:2312.10628* (2023).
  - [49] Linji Wang, Zifan Xu, Peter Stone, and Xuesu Xiao. 2024. Grounded curriculum learning. *arXiv preprint arXiv:2409.19816* (2024).
  - [50] Yin Wang, Mu Li, Jiapeng Liu, Zhiying Leng, Frederick WB Li, Ziyao Zhang, and Xiaohui Liang. 2025. Fg-T2M++: LLMs-Augmented Fine-Grained Text Driven Human Motion Generation. *arXiv preprint arXiv:2502.05534* (2025).
  - [51] Zan Wang, Yixin Chen, Baoxiong Jia, Puhao Li, Jinlu Zhang, Jingze Zhang, Tengyu Liu, Yixin Zhu, Wei Liang, and Siyuan Huang. 2024. Move as you say interact as you can: Language-guided human motion generation with scene affordance. In *Proceedings of the IEEE/CVF Conference on Computer Vision and Pattern Recognition*. 433–444.
  - [52] Zhiming Wang, Ning Ge, and Jianhua Lu. 2025. Motion In-betweening with Spatial and Temporal Transformers. *IEEE Transactions on Circuits and Systems for Video Technology* (2025), 1–1. doi:10.1109/TCSVT.2025.3526236
  - [53] Yiming Xie, Varun Jampani, Lei Zhong, Deqing Sun, and Huaizu Jiang. 2024. OmniControl: Control Any Joint at Any Time for Human Motion Generation. *arXiv:2310.08580* [cs.CV] <https://arxiv.org/abs/2310.08580>
  - [54] Ling Yang, Zhilong Zhang, Yang Song, Shenda Hong, Runsheng Xu, Yue Zhao, Wentao Zhang, Bin Cui, and Ming-Hsuan Yang. 2023. Diffusion models: A comprehensive survey of methods and applications. *Comput. Surveys* 56, 4 (2023), 1–39.
  - [55] Zhuoyi Yang, Jiayan Teng, Wendi Zheng, Ming Ding, Shiyu Huang, Jiazheng Xu, Yuanming Yang, Wenyi Hong, Xiaohan Zhang, Guanyu Feng, et al. 2024. Cogvideox: Text-to-video diffusion models with an expert transformer. *arXiv preprint arXiv:2408.06072* (2024).
  - [56] Ziming Cheng Jiangfeiyang Wang Yihao Liao, Yiyu Fu. 2024. AnimationGPT: An AIGC tool for generating game combat motion assets. <https://github.com/fyyakaxy/AnimationGPT>.
  - [57] Bowen Zhang, Yidong Wang, Wenxin Hou, Hao Wu, Jindong Wang, Manabu Okumura, and Takahiro Shinozaki. 2021. Flexmatch: Boosting semi-supervised learning with curriculum pseudo labeling. *Advances in neural information processing systems* 34 (2021), 18408–18419.
  - [58] Jianrong Zhang, Yangsong Zhang, Xiaodong Cun, Yong Zhang, Hongwei Zhao, Hongtao Lu, Xi Shen, and Ying Shan. 2023. Generating human motion from textual descriptions with discrete representations. In *Proceedings of the IEEE/CVF conference on computer vision and pattern recognition*. 14730–14740.
  - [59] Mingyuan Zhang, Huirong Li, Zhongang Cai, Jiawei Ren, Lei Yang, and Ziwei Liu. 2023. Finemogen: Fine-grained spatio-temporal motion generation and editing. *Advances in Neural Information Processing Systems* 36 (2023), 13981–13992.
  - [60] Xuan Zhang, Pamela Shapiro, Gaurav Kumar, Paul McNamee, Marine Carpuat, and Kevin Duh. 2019. Curriculum learning for domain adaptation in neural machine translation. *arXiv preprint arXiv:1905.05816* (2019).
  - [61] Zeyu Zhang, Yiran Wang, Wei Mao, Danning Li, Rui Zhao, Biao Wu, Zirui Song, Bohan Zhuang, Ian Reid, and Richard Hartley. 2025. Motion Anything: Any to Motion Generation. *arXiv preprint arXiv:2503.06955* (2025).
  - [62] Yangyang Zhao, Zhenyu Wang, and Zhenhua Huang. 2021. Automatic curriculum learning with over-repetition penalty for dialogue policy learning. In *Proceedings of the AAAI Conference on Artificial Intelligence*, Vol. 35. 14540–14548.
  - [63] Xukun Zhou, Fengxin Li, Ming Chen, Yan Zhou, Pengfei Wan, Di Zhang, Hongyan Liu, Jun He, and Zhaoxin Fan. 2025. ExGes: Expressive Human Motion Retrieval and Modulation for Audio-Driven Gesture Synthesis. *arXiv preprint arXiv:2503.06499* (2025).
  - [64] Wentao Zhu, Xiaoxuan Ma, Dongwoo Ro, Hai Ci, Jinlu Zhang, Jiaxin Shi, Feng Gao, Qi Tian, and Yizhou Wang. 2023. Human motion generation: A survey. *IEEE Transactions on Pattern Analysis and Machine Intelligence* 46, 4 (2023), 2430–2449.